Civil and Environmental Engineering
Vol. 0, Issue 0, DOI: 10.2478/cee-2026-0052

The Effect of Polyaluminum Chloride (PAC) Residue on the Mechanical Properties and Freeze-Thaw Resistance of Cement Mortar

Ming YAO[1], Huan LIAN[2,*], Shaoqiang CHAI[1], Hai SHANG[1], Tianchu FENG[1]

[1] The Seventh Engineering Co., Ltd. of CFHEC, Zhengzhou, Henan 451450, China.

[2] College of Civil Engineering, Henan Polytechnic University, Jiaozuo, Henan 454003, China.

* corresponding author: 1669565062@qq.com

Date of Submission: 13 September 2025
Revision Date: 16 October 2025
Date of Acceptance: 18 October 2025

Civil and Environmental Engineering
Journal of the Faculty of Civil Engineering | University of Žilina

Abstract

The accumulation of polyaluminium chloride (PAC) residue seriously restricts the sustainable development of water purification agent industry. This study proposes the utilization of PAC residue as a mineral admixture in cement-based materials, systematically investigates its effects on the physical, mechanical, and frost resistance properties of cement mortar, and employs scanning electron microscopy (SEM) microstructural analysis to elucidate the underlying mechanisms. The experimental results demonstrate that increasing PAC residue content leads to a gradual reduction in mortar workability, while the 7-day compressive strength exhibits a steady decline with the increment of PAC residue content. At a PAC residue content of 5%, the material exhibits optimal compressive strength at 28-day and 56-day curing ages, achieving 26.6 MPa and 29.1 MPa, respectively. Additionally, at 5% PAC residue content, the pore structure parameters of the mortar reach their optimal values, while the frost resistance achieves the highest level. SEM analysis demonstrates that a modest incorporation of PAC waste residue effectively fills the internal pores of mortar, thereby enhancing matrix compactness. Furthermore, the active components in PAC waste residue participate in secondary reactions with cement hydration products, optimizing both the composition and distribution of hydration phases to refine the mortar's microstructure.

Keywords

PAC residue; Cement mortar; Compressive strength; Pore structure; Frost resistance.

1. Introduction

With rapid economic development, environmental challenges have become increasingly prominent. Consequently, research on the accumulation and resource upcycling of industrial by-products has emerged as a critical focal point. The utilization of industrial waste in construction materials represents an indispensable pathway toward green and low-carbon development (Atiea, 2025). Polyaluminum chloride (PAC) is a high-efficiency water purification agent (Li, 2022; Wu, 2020) possessing high adsorption capacity, large floc formation (Matsui, 2017; Ghafari, 2010), rapid settling velocity, and strong adaptability (Tania, 2009; Singh, 2010), and is widely applied in wastewater treatment applications

(Shirasaki, 2014; Xue, 2018). Numerous production methods exist for PAC (Zouboulis, 2010; Zakaria, 2020; Li,2022) , with the most common involving a two-step acid leaching process: bauxite and calcium aluminate powder react with hydrochloric acid or mixed acids to produce liquid PAC, while the precipitated solids form acidic viscous residue (Zouboulis, 2010). However, prevailing waste residue disposal methods—predominantly landfill disposal and stockpiling—pose significant contamination risks to soil strata and underlying aquifers. According to relevant research (Li, 2022), the chemical composition of the treated PAC waste residue includes SiO2, Al2O3 and CaO, and has certain pozzolanic activity (Krivenko, 2017; Manfroi,2013; Wijaya, 2024).

Currently, industrial waste slag with pozzolanic activity as the admixture of cement-based products is an effective way of efficient resource utilization of waste slag. Cheng et al. (2016) and Wong et al. (2004) demonstrated that the incorporation of mine tailings effectively fills matrix pores, optimizes microstructure, and thereby enhances mortar strength. Ghalehnovi et al.(2019; 2019) found that an optimal proportion of red mud regulates concrete rheological properties, reducing free water content while simultaneously improving durability. Ortega et al. (2019) further demonstrated that the incorporation of red mud promotes the refinement of mortar microstructure. Manfroi et al. (2014) experimentally determined that a 5% red mud replacement serves as the optimal dosage. Matos et al. (2018) and Steiner et al. (2015) demonstrated that ceramic polishing powder at a 20% replacement rate simultaneously enhances flowability without compromising strength. Liu & Wang (2017) further confirmed that steel slag-silica fume composite admixtures significantly refine the pore structure of cement-based materials. The synergistic effect between silica fume's early pozzolanic activity and steel slag's sustained hydration characteristics promotes C-S-H gel densification, drastically reducing the proportion of harmful pores.

Studies demonstrate that the incorporation of industrial by-products with pozzolanic activity significantly enhances the freeze-thaw durability of cement-based materials through the refinement of their pore structure (Nemec, 2024; Peknikova, 2025). Sun et al. (2022) demonstrated through rapid freezing tests that the pozzolanic reaction products of self-coal gangue powder effectively reduce mortar porosity, thereby enhancing its freeze-thaw resistance. Meanwhile, Jin et al. (2024) found that under low water-to-cement ratios, the incorporation of fly ash significantly decreases the percentage of harmful pores after freeze-thaw cycles, improving the mortar's resistance to such cycles. Xu et al. (2024; 2024; 2025) systematically investigated the influence of PAC residue on the performance of cement-based materials, demonstrating that a low dosage of PAC residue significantly enhances the freeze-thaw resistance of concrete masonry units. Meanwhile, Yang et al. (2022) proposed that PAC residue primarily functions as a micro-aggregate, filling mortar pores and improving material strength at low replacement rates.

The review above shows that the mechanical properties of mortar can be improved by refining its microstructure through adding an appropriate amount of PAC waste residue. This study utilized PAC residue subjected to acid- and chloride-removal pretreatment, processed via drying and grinding to prepare a modified admixture. It systematically investigated its underlying mechanisms in the mechanical properties, pore structure characteristics, and freeze-thaw durability of mortar. Based on experimental results, this study proposes the optimal dosage range and recommended process parameters of PAC residue in cement mortar, aiming to provide a scientific basis for its resourceful utilization in the construction materials sector.

2. Methodology

2.1. Materials

The experiment employed P.O42.5 ordinary Portland cement. The fine aggregate used was river sand with a fineness modulus of 2.4, a maximum grain size of 1.18 mm, and a mass absorption rate of 0.91%, As shown in Figure 1. PAC residue, a by-product of coagulant production in industrial processes, exhibits a density of 2.231 g/cm^3 at ambient temperature. Due to its weak acidic nature, it cannot be directly utilized as a cementitious admixture. Prior to experimentation, the PAC residue underwent acid-removal pretreatment, and its specific preparation process is illustrated

in Figure 2. PAC residue in its raw blocky form was subjected to drying, crushing, screening, and milling processes to prepare PAC residue samples with specific particle size distributions (0–0.075 mm) for experimental investigation. The XRD diffractogram of PAC residue is presented in Figure 3. Figure 4 reveals the microscopic morphology of PAC waste residues, exhibiting heterogeneous particle size distribution, angular fragment morphology, and roughened surfaces with abundant micropores.

Figure 1: Fine aggregate

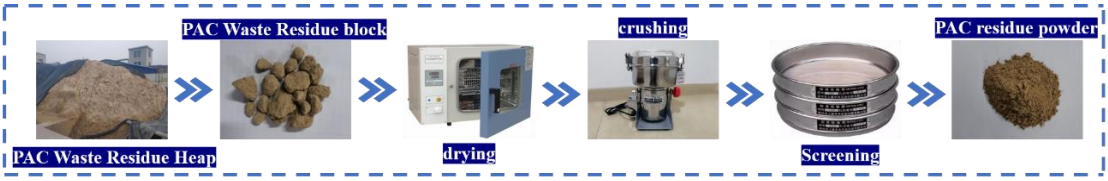

Figure 2: Preparation process of PAC waste residue particles

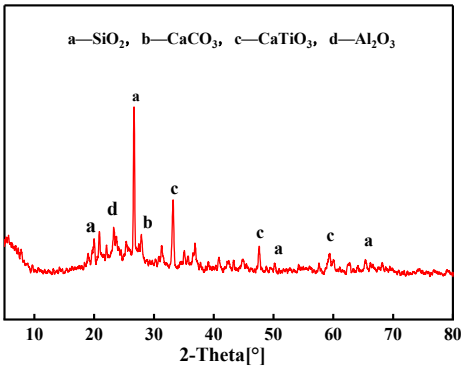

Figure 3: XRD diffraction pattern of PAC waste residue

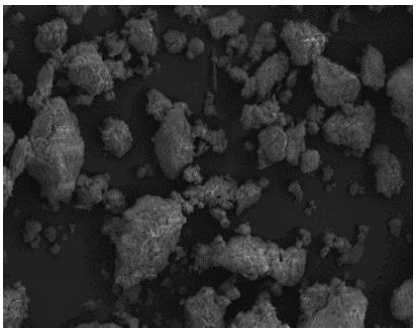

Figure 4: Microscopic morphology of PAC waste residue

Figure 5 presents the particle size interval distribution and cumulative distribution of cement and processed PAC residue after grinding and sieving. The granulometric analysis reveals that PAC residue and cement exhibit similar particle size distribution curves, with cement particles demonstrating a marginally smaller mean particle size compared to PAC residue particles.

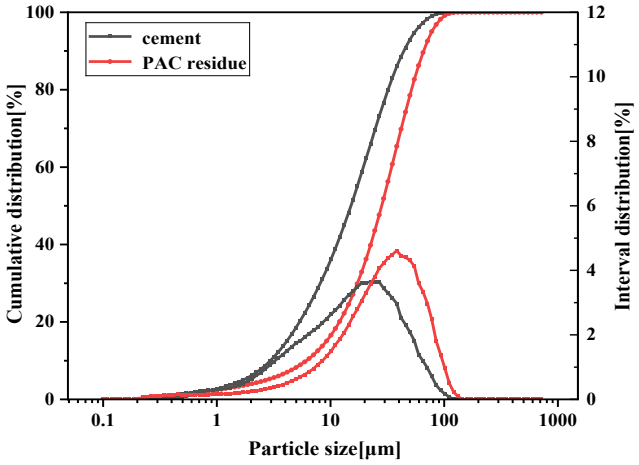

Figure 5: Particle size distribution curves of cement and PAC waste residues

2.2. Mix ratio and specimen preparation

During the preliminary testing phase, the water demand of PAC residue was pre-determined following the procedures specified in the Chinese National Standard GB/T 18736-2017. In this experiment, a relatively high water-binder ratio of 0.8 was employed while maintaining a constant paste volume fraction of 45%. Five comparative groups were established using the mass replacement method: a control group (0% replacement) and experimental groups with PAC residue replacing 5%, 10%, 15%, and 20% of the cement content. The specific material proportions for each mix design are detailed in Table 1.

Table 1: Mortar mix proportion

Serial number [-]	Cement [kg/m^3]	Water [kg/m^3]	PAC residue [kg/m^3]	Sand [kg/m^3]
PACM0	402.0	323	0	1411
PACM5	381.9	323	20.1	1411
PACM0	361.8	323	40.2	1411
PACM15	341.7	323	60.3	1411
PACM20	321.6	323	80.4	1411

During mortar preparation, PAC waste residue dry powder is initially mixed with cement for 1 minute to ensure thorough homogenization and uniform dispersion. Subsequently, the mixture is blended with an aqueous solution containing water and superplasticizer for 1 minute. Finally, fine aggregate is incorporated and mixed for 2 minutes to achieve complete integration. The mixed mortar is cast into molds and placed in a standard curing cabinet with temperature maintained at 20±2°C and relative humidity exceeding 90% throughout curing. Covered with plastic film to prevent condensate from dripping and damaging the specimens. After 24 hours of curing, the specimens were demolded and labeled, and subsequently continued to be cured in the standard environment until reaching the designated curing ages for testing.

2.3. Test method

1. Mortar consistency and compression test

The mortar consistency and compressive strength tests were conducted in accordance with JGJ/T70-2009 standard. After curing to the designated ages, the standard cubic specimens (70.7 mm × 70.7 mm × 70.7 mm) were subjected to compressive strength testing using a 1000kN microcomputer-controlled hydraulic testing machine. The loading rate was maintained at 1kN/s. For each curing age group, three replicate specimens are prepared, and the average value is adopted as the final test result.

2. Mortar pore Structure test

Standard cubic specimens were subjected to 28-day standard curing and subsequently dried to constant mass at 105±5℃. During testing, the specimens were immersed in water, and their wet masses (m0.25h, m1h, and m24h) were measured at three characteristic time points: 0.25 hours, 1 hour, and 24 hours. Finally, the maximum water absorption rate (Wmax), pore size uniformity coefficient (α), and mean pore diameter (λ) were calculated using Equations (1) and (2) of the sorption kinetics model (Chen,1989). The correction term in the model accounts for the dual-pathway water absorption mechanism specific to cement-based materials, involving capillary and gel pores.

$$W_t = W_{max}(1 - \mathrm{e}^{-\lambda_1 t^{\alpha}}) \quad (1)$$

$$W_t = W_{max}(1 - e^{-(\lambda_1 t)^{\alpha}}) \quad (2)$$

Where*:*

W_t - definition of the mass-based water absorption rate (%) of the specimen after t hours,

W_{max} - definition of the maximum mass-based water absorption rate,

λ - definition of the average pore diameter of capillary pores, The λ value is calculated as the arithmetic mean of λ_1 and λ_2, and a larger λ value indicates a greater average pore diameter

α - definition of the uniformity of capillary pore sizes, with values ranging from 0 to 1. A higher α value indicates greater pore size uniformity, and α=1 signifies a single-capillary pore structure in mortar.

The expression for W in Equations (1) and (2) is given by Equation (3):

$$\mathrm{W_t} = \frac{\mathrm{m_t} - \mathrm{m_0}}{\mathrm{m_0}} \quad (3)$$

Where*:*

m_t - definition of the mass of the specimen after soaking for t hours [g]

m_0 - definition of the mass after drying [g].

The expression for α in Equations (1) and (2) is given by Equation (4):

$$(x + a)^n \alpha = \frac{\ln\left[\frac{\ln\left(1 - \frac{\mathrm{W_{t2}}}{\mathrm{W_{max}}}\right)}{\ln\left(1 - \frac{\mathrm{W_{t1}}}{\mathrm{W_{max}}}\right)}\right]}{\ln\left(\frac{\mathrm{t_2}}{\mathrm{t_1}}\right)} \quad (4)$$

When t1=0.25 and t2=1, the value of α can be calculated.

When t=1 in Equation (1), the value of λ1 can be calculated as shown in Equation (5).

$$(x + a)^n \lambda_1 = \ln\left(\frac{\mathrm{W_{max}}}{\mathrm{W_{max}} - \mathrm{W_1}}\right) \quad (5)$$

When t=0.25, the value of λ2 can be calculated by substituting α into Equation (2).

3. Freeze-thaw resistance test

In accordance with the provisions of JGJ/T70-2009 for mortar freeze-thaw resistance testing, the specimens were subjected to freeze-thaw cycle testing after reaching a 28-day curing age. After every five freeze-thaw cycles, appearance inspection, mass measurement, and compressive strength determination were conducted. For each mix proportion at specified numbers of freeze-thaw cycles, three replicate specimens are tested, and the average value is adopted as the final test result to assess durability performance under repeated freeze-thaw actions.

4. Scanning electron microscope (SEM) test

The microstructural characterization of the specimens was conducted using a Zeiss Merlin Compact field emission scanning electron microscope. Upon reaching a 28-day curing age, cylindrical specimens with diameters ranging from 5 mm to 10 mm were extracted from the central region of the mortar. Immediately after sampling, the specimens were immersed in absolute ethanol to stop hydration and stored under sealed conditions. Prior to testing, the mortar specimens were retrieved and subjected to drying treatment.

3. Discussion Results and Discussion

3.1. mortar consistency

The influence of PAC residue on mortar flow properties is illustrated in Figure 6, showing that mortar consistency gradually decreases with increasing PAC residue content. When PAC content increases from 5% to 20%, mortar consistency reduces from 88 mm to 75 mm, and mortar flowability decreases by 3.30% to 17.58% compared to the reference group without PAC residue. This change primarily originates from the physical characteristics of PAC residue: its irregular particle morphology increases internal frictional resistance within the system, thereby elevating water demand; simultaneously, the porous surface structure adsorbs free water, reducing the effective water-to-binder ratio and consequently diminishing mortar flowability.

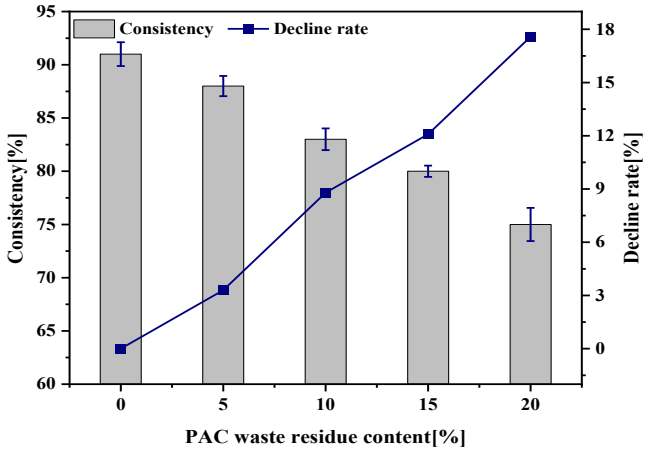

Figure 6: Effect of PAC residue content on mortar consistency

3.2. Compressive strength

Figure 7 illustrates the variation in compressive strength and compressive strength ratio of mortar incorporating PAC residue across different curing ages. The compressive strength ratio is defined as the ratio of the compressive strength of each group to that of the reference group without PAC residue, primarily aiming to more intuitively reflect the impact of PAC residue on mortar compressive strength. It can be observed that PAC residue exerts an adverse effect on the early compressive strength of mortar, with the 7-day compressive strength exhibiting a decreasing trend as PAC

residue content increases. Specifically, compared to the reference group without PAC residue (compressive strength: 18.5 MPa), the strengths of mortar specimens with PAC residue contents of 5%, 10%, 15%, and 20% were 17.8 MPa, 16.9 MPa, 15.5 MPa, and 13.8 MPa, respectively, corresponding to strength reduction rates of 3.78%, 8.65%, 16.22%, and 25.41%. This is attributed to the larger particle size of PAC residue, which slows down the hydration reactions of cement (Hansen, 2020), thereby impeding the early strength development of mortar.

However, by comparing the compressive strength of mortar at 14-day and 28-day curing ages, it is observed that the compressive strength exhibits an initial increase followed by a subsequent decrease with increasing PAC residue content. Peaking at 5% incorporation, with strength gains of 3.50% and 2.47% relative to the reference group at 14-day and 28-day curing ages, respectively. This is attributed to the micro-filler effect of a low PAC residue content, which effectively fills internal pores and optimizes the pore structure of mortar, thereby facilitating the development of later-age strength. It is noteworthy that even at a PAC residue content of 10%, the 28-day and 56-day compressive strengths of the mortar remain comparable to the reference group, indicating that within this dosage range, the mortar's later-age strength performance can still reach or even exceed that of conventional mortar. Therefore, the moderate incorporation of PAC residue can maintain or enhance the long-term mechanical properties of mortar to a certain extent. Concurrently, experimental observations demonstrated that all specimens exhibited brittle failure characterized by sudden fragmentation along dominant shear planes, with no statistically significant variations observed across mix proportions, thereby establishing that PAC waste residue incorporation does not alter the fundamental failure mechanism of the mortar.

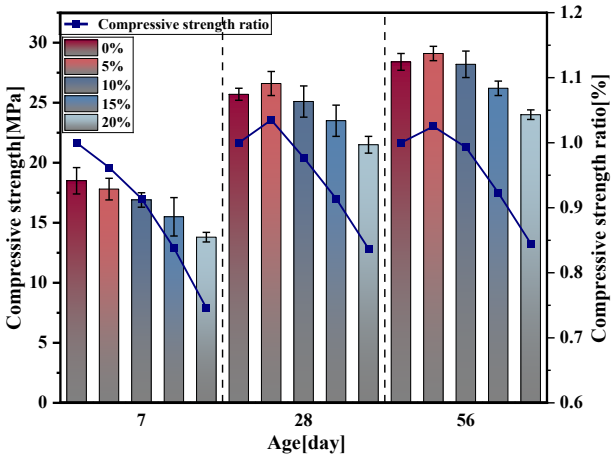

Figure 7: Compressive strength and compressive strength ratio of mortar

3.3. Mortar pore structure parameters

According to the test data, the influence of the law of PAC waste residue content on mortar mass water absorption W_{max}, pore uniformity coefficient α and average pore diameter λ is drawn as shown in Figure 8.

As shown in Figure 8, the influence of PAC residue content on mortar pore structure exhibits a distinct nonlinear relationship: at the optimal 5% PAC residue content, the system simultaneously achieves synergistic optimization of three critical parameters. Specifically, water absorption is reduced to 0.119 (an 8.3% decrease compared to the reference group), the pore size uniformity coefficient is enhanced to 0.686 (1.12 times the peak value of the reference group), and the average pore size is reduced to 0.686 μm (a 4.3% decrease relative to the reference group). As PAC residue content continues to increase, the mortar's water absorption and pore size parameters exhibit synchronized deterioration, indicating the presence of a critical dosage effect in the optimization of mortar pore structure by PAC residue. When PAC residue content is below 5%, its active components react with cement hydration products to effectively fill transition pores. Simultaneously, PAC residue particles act as a micro-graded medium, improving the pore structure and enhancing mortar

density. However, excessive PAC residue replacement of cement leads to a reduction in hydration product formation, resulting in an increase internal microcrack density and subsequent deterioration of the pore structure.

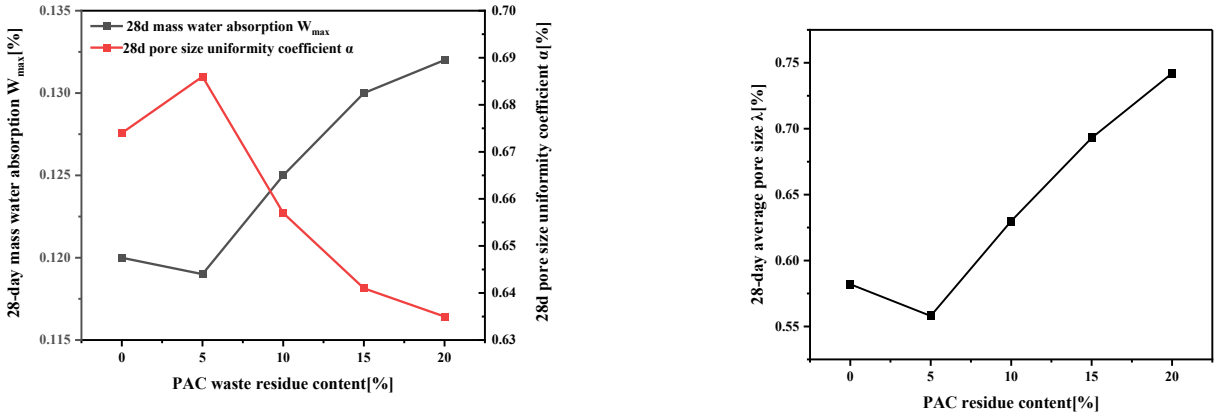

a) b)

Figure 8: Effect of PAC waste residue content on the structural parameters of mortar pores: a) 28-day mass water absorption and pore size uniformity coefficient; b) 28-day average pore size

3.4. Freeze-thaw resistance

1. Mass loss

The experimental results showing the mass loss rate of PAC residue-containing mortar specimens as the number of freeze-thaw cycles increases are presented in Figure 9.

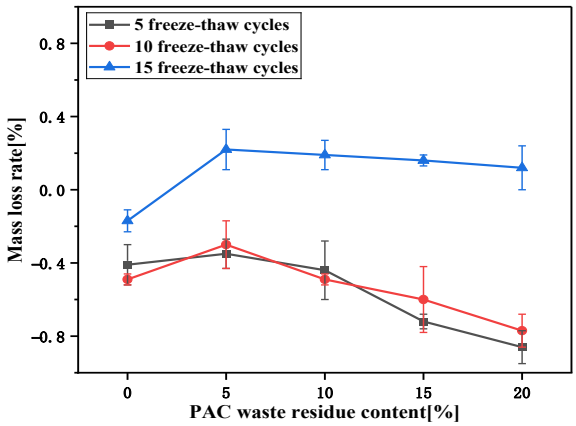

Figure 9: Mass loss rate

As illustrated in Figure 9, during the initial phase of freeze-thaw cycles, pore water freezing-induced expansion generates microcracks, leading to increased water absorption and temporary mass gain. However, as the freeze-thaw cycle progresses, the degradation of the interfacial transition zone (ITZ) and progressive matrix disintegration result in a gradual increase in the mass loss rate of mortar specimens. Upon reaching 15 freeze-thaw cycles, all mortar groups incorporating PAC waste residue exhibited mass loss, except the reference group. As shown in Figure 10, progressive surface deterioration manifested as increasing roughness, pitting, spalling, and corner breakage with escalating freeze-thaw cycles. This degradation was further exacerbated by through-crack formation, intensifying overall mass loss.

During the initial phase of freeze-thaw cycles, the mass loss rate of low-admixture groups (≤5%) is lower than that of the reference group, which is attributed to the optimized pore structure's inhibition of moisture migration. When the

number of freeze-thaw cycles reaches 15, the high-dosage groups (>5%) exhibit an anomalous decrease in mass loss rate. The fundamental cause lies in the increased water-to-binder ratio resulting from PAC residue replacing cement. Unreacted PAC residue particles act as aggregates while maintaining internal relative humidity through their high-water absorption capacity. Although this phenomenon temporarily delays apparent mass loss, it accelerates durability degradation by promoting microcrack propagation.

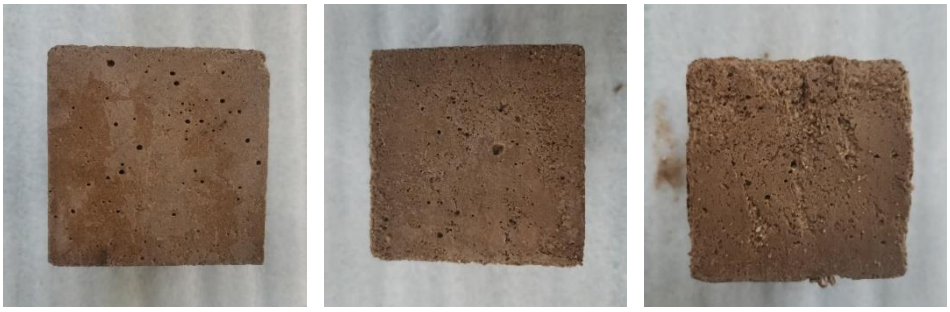

Figure 10: Failure mode of the mortar freeze-thaw cycle test

2. Compressive Strength Loss

As illustrated in Figure 11, the compressive strength loss rate of mortar specimens after freeze-thaw damage exhibits a variation trend dependent on PAC residue content and the number of freeze-thaw cycles. The experimental results demonstrate that as the number of freeze-thaw cycles increases, the degree of damage inflicted on the specimens gradually intensifies. The PAC residue content exhibits a significant dose-dependent effect on mortar freeze-thaw damage. For the 5% dosage group, the compressive strength loss rates after 5, 10, and 15 freeze-thaw cycles are 16.70%, 32.71%, and 47.13%, respectively. In contrast, the 20% dosage group demonstrates increased loss rates of 20.44%, 40.67%, and 60.93%. Its deterioration rate increased by 60.5%. This is attributed to the hydrophilic reaction of PAC residue, which possesses a strong water absorption capacity. The absorbed moisture undergoes volume expansion during freezing, exerting pressure on the internal structure and causing damage. Furthermore, the increased internal moisture content amplifies freeze-thaw pressure, exacerbating specimen deterioration [26]. Consequently, as the PAC residue content increases, the compressive strength loss rate of mortar specimens becomes more pronounced due to intensified microcrack propagation.

Notably, when PAC residue content is 5%, the compressive strength loss rates after 5, 10, and 15 freeze-thaw cycles are reduced by 0.4%, 1.09%, and 1.3%, respectively, compared to the reference group without PAC residue. This indicates that partial cement replacement with PAC residue (≤5%) optimizes the pore structure of cementitious matrices by refining pore connectivity and reducing capillary porosity, thereby enhancing freeze-thaw resistance.

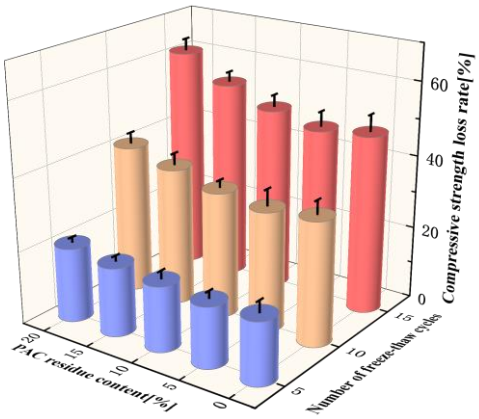

Figure 11: Compressive strength loss rate

3.5. Microstructure analysis

To investigate the influence mechanisms of PAC residue content on the microstructure and hydration products of mortar specimens, SEM analysis was conducted on three groups of mortar specimens with different PAC residue contents (0%, 5%, and 20%). All specimens were sampled at the 28-day curing age to ensure complete hydration. Figure 12 presents SEM micrographs magnified at 1000× and 5000×, respectively, illustrating the microstructural characteristics of the three groups of specimens with varying PAC residue contents (0%, 5%, and 20%).

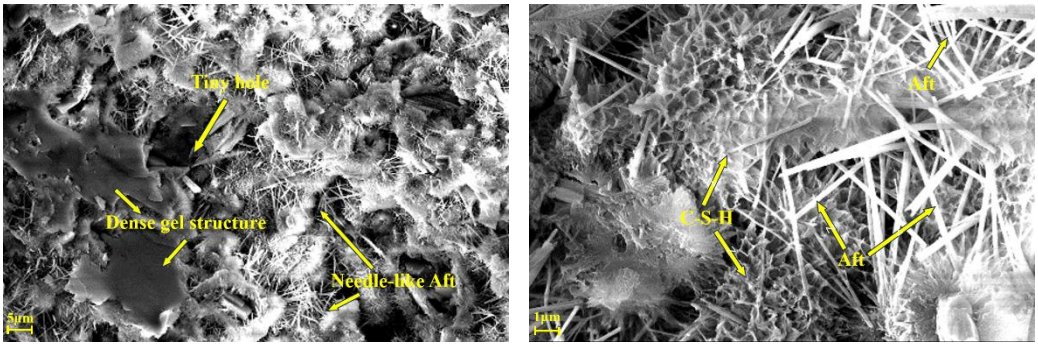

a) 0%

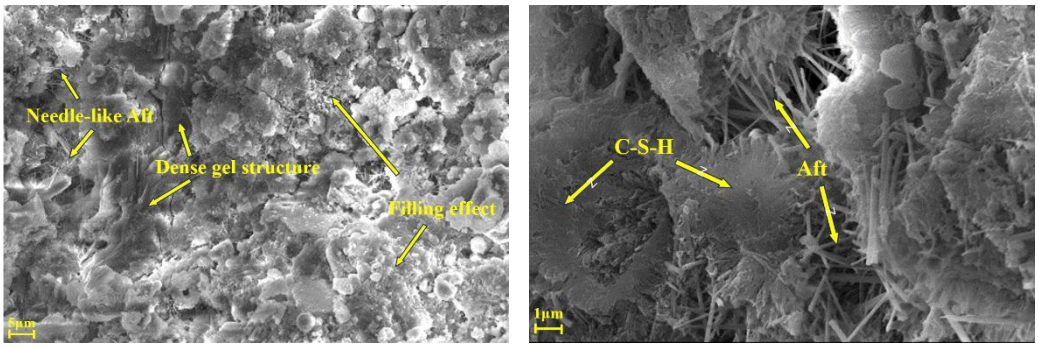

b) 5%

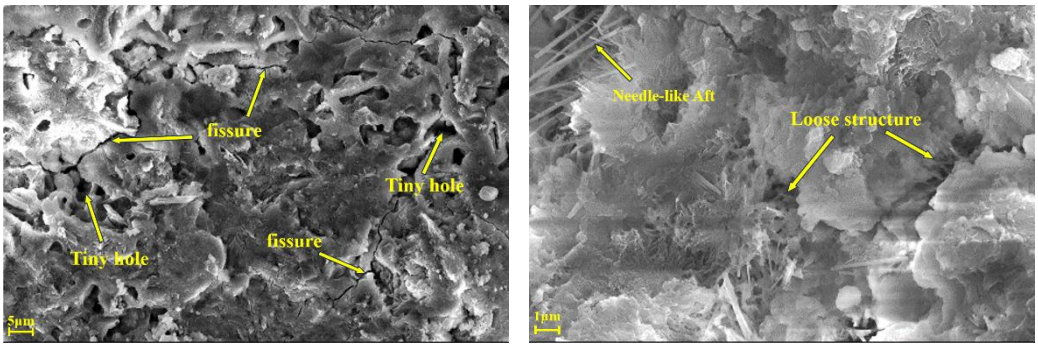

c) 20%

Figure 12: Microstructure of mortar under different PAC waste residue contents

As shown in Fig. (a), the PAC-free mortar exhibits a typical hydrate distribution: The matrix is densely interwoven with a network of calcium silicate hydrate (C-S-H) and needle-shaped ettringite (Aft), forming a continuous skeleton that results in a relatively dense structure. However, high-resolution SEM observations reveal the presence of micropores within this system, which may serve as potential initiation sites for freeze-thaw damage.

Microstructural analysis of Fig. (b) indicates that at 5% PAC waste residue incorporation, the quantity and morphological characteristics of AFt crystals in the mortar system are highly consistent with those of the reference group, demonstrating that PAC waste residue does not disrupt the aluminate-phase-dominated initial hydration pathway. Notably, the mortar incorporating 5% PAC waste residue exhibits a more compact microstructure: significantly enhanced matrix continuity, substantially reduced porosity, and an absence of discernible crack defects. Notably, mortar specimens incorporating 5% PAC residue exhibit a more compact microstructure characterized by a continuous matrix without cracks, significantly reduced porosity, and no apparent defects. This phenomenon arises from the dual optimization mechanisms of PAC residue: On the one hand, a small amount of PAC waste residue particles can effectively fill the internal pores of mortar, reducing pore connectivity; on the other hand, its reactive components undergo secondary hydration reactions with cement hydration by-products $Ca(OH)_2$, generating additional calcium silicate hydrate C-S-H gel to refine the pore structure. The optimized microstructure exhibits excellent consistency with macroscopic performance enhancements, including elevated compressive strength and mitigated strength loss rate under freeze-thaw cycles, thereby elucidating the durability-enhancing mechanisms of PAC waste residue in mortar through a multiscale analysis.

As depicted in Figure (c), when PAC residue content reaches 20%, excessive PAC incorporation induces observable microstructural degradation: a substantial reduction in AFt crystal quantity combined with insufficient hydration products disrupts matrix continuity, resulting in a porous and loosely packed microstructure characterized by increased interparticle gaps. This phenomenon arises because excessive PAC dilutes the concentration of cement clinker, inhibits the formation of hydration products, and thus compromises the cementitious capability of the system. As the majority of unreacted PAC residue remains inert filler material, occupying spaces that would otherwise be filled by hydration products, the mortar matrix becomes increasingly loose and porous. Consequently, excessive PAC residue exerts detrimental effects on both compressive strength and frost resistance.

In summary, with a 5% PAC waste residue incorporation, the cement-based material achieves optimal mechanical properties and freeze-thaw resistance, demonstrating significant superiority over the reference group. This dosage effectively optimizes pore structure parameters and yields a denser microstructure, confirming its engineering applicability.

4. Conclusion

This study systematically investigates the synergistic influence mechanisms of PAC residue dosages on the macroscopic properties and microstructure of cement mortar, with primary findings summarized as follows:

(1) The mortar consistency decreases with increasing PAC residue content, exhibiting a more pronounced decline at higher dosages. While PAC residue inhibits early-stage cement hydration, a moderate dosage optimizes long-term compressive strength development. Specifically, the 28-day and 56-day compressive strengths peak at 5% PAC residue content, reaching 26.6 MPa and 29.1 MPa, respectively.

(2) At 5% PAC residue content, the pore structure parameters of the mortar reach their optimal values, while the mass loss and compressive strength degradation after freeze-thaw cycles are both lower than those of the reference group without PAC residue addition.

(3) SEM analysis demonstrates that moderate PAC residue replacement does not significantly reduce hydration products but instead effectively fills micro-cracks in the cement matrix, enhancing the overall compaction of the structure. Additionally, PAC residue can undergo secondary hydration reactions with cement hydration products, thereby improving the internal pore structure of mortar and enhancing its strength and durability.

Acknowledgements

Financial supports from the National Natural Science Foundation of China (No. 52478250), and the Science and Technology Project of Henan Transportation Investment Group Co., Ltd. (No. HNJT2024–11) are gratefully appreciated.

Author Contributions

M.Y. designed the study and supervised the project. **H.L.** contributed to data interpretation and manuscript drafting. **Sq.C.** conducted the experiments and collected the data. **H.S.** contributed to manuscript writing. **Tc.F.** Carried out translation work. All authors critically reviewed and approved the final version of the manuscript and agreed to be accountable for all aspects of the work.

Disclosure of Interest

The authors declare that they have no known competing financial interests or personal relationships that could have appeared to influence the work reported in this paper.

Data Availability Statement

The data supporting the findings of this study are available from the corresponding author upon reasonable request.

References

Atiea H M, Albahrani H S, Allaban M F, et al. (2025). Ceramic Waste as Fine and Coarse Aggregates for Sustainable Environment and Fire-Resistant Buildings. Civil and Environmental Engineering, 28(1): 535-544. https://doi.org/10.2478/cee-2025-0040

Li C, Song Z, Zhang W, et al. (2022). Impact of hydroxyl aluminum speciation on dewaterability and pollutants release of dredged sludge using polymeric aluminum chloride. Journal of Water Process Engineering, 49: 103051. https://doi:10.1016/j.jwpe.2022.103051.

Wu Z, Zhang X, Pang J, et al. (2020). High-poly-aluminum chloride sulfate coagulants and their coagulation performances for removal of humic acid. RSC advances, 10(12): 7155-7162. https://doi:10.1039/C9RA10189F.

Matsui Y, Shirasaki N, Yamaguchi T, et al. (2017). Characteristics and components of poly-aluminum chloride coagulants that enhance arsenate removal by coagulation: Detailed analysis of aluminum species. Water research, 118: 177-186. https://doi:10.1016/j.watres.2017.04.037.

Ghafari S, Aziz H A, Bashir M J K. (2010). The use of poly-aluminum chloride and alum for the treatment of partially stabilized leachate: A comparative study. Desalination, 257(1-3): 110-116. https://doi:10.1016/j.desal.2010.02.037.

Tania Chatterjee, Sudipta Chatterjee, Dae S Lee, et al.(2009). Coagulation of soil suspensions containing nonionic or anionic surfactants using chitosan, polyacrylamide, and polyaluminium chloride .Chemosphere, 75 (10):1307-1314. https://doi:10.1016/j.chemosphere.2009.03.012.

Singh S S, & Dikshit A K. (2010). Optimization of the parameters for decolourization by Aspergillus niger of anaerobically digested distillery spentwash pretreated with polyaluminium chloride. Journal of Hazardous Materials, 176(1-3): 864-869. https://doi:10.1016/j.jhazmat.2009.11.116

Shirasaki N, Matsushita T, Matsui Y, et al. (2014). Improved virus removal by high-basicity polyaluminum coagulants compared to commercially available aluminum-based coagulants.Water Research, 48(jan.1):375-386. https://doi:10.1016/j.watres.2013.09.052.

Xue M, Gao B, Li R, et al. (2018). Aluminum formate(AF): Synthesis, characterization and application in dye wastewater treatment. Journal of Environmental Sciences,74: 95-106. https://doi:10.1016/j.jes.2018.02.013

Zouboulis A I, & Tzoupanos N. (2010). Alternative cost-effective preparation method of polyaluminium chloride (PAC) coagulant agent: Characterization and comparative application for water/wastewater treatment. Desalination, 250(1): 339-344. https://doi:10.1016/j.desal.2009.09.053.

Zakaria Z A, & Ahmad W A. (2020). Organic and Inorganic Matter Removal Using High Polymeric Al 13 Containing Polyaluminium Chloride. Water, Air, & Soil Pollution, 231: 1-10. https://doi:10.1007/s11270-020-04706-8.

Li F, Jiang J Q, Wu S, et al. (2010). Preparation and performance of a high purity poly-aluminum chloride. Chemical Engineering Journal, 156(1): 64-69. https://doi:10.1016/j.cej.2009.09.034

Li Q, Zhang J, Gao J, et al. (2022). Preparation of a novel non-burning polyaluminum chloride residue (PACR) compound filler and its phosphate removal mechanisms. Environmental science and pollution research, 29: 1532-1545. https://doi:10.1007/s11356-021-15724-2.

Krivenko P, Kovalchuk O, Pasko A, et al. (2017). Development of alkali activated cements and concrete mixture design with high volumes of red mud. Construction and Building Materials, 151: 819-826. https://doi:10.1016/j.conbuildmat.2017.06.031.

Cheng Y, Huang F, Li W, et al. (2016). Test research on the effects of mechanochemically activated iron tailings on the compressive strength of concrete. Construction and Building Materials, 118: 164-170. https://doi:10.1016/j.conbuildmat.2016.05.020.

Wong R C K, Gillott J E, Law S, et al. (2004). Calcined oil sands fine tailings as a supplementary cementing material for concrete. Cement and concrete research, 34(7): 1235-1242. https://doi:10.1016/j.cemconres.2003.12.018.

Ghalehnovi M, Roshan N, Hakak E, et al. (2019). Effect of red mud (bauxite residue) as cement replacement on the properties of self-compacting concrete incorporating various fillers. Journal of Cleaner Production, 240: 118213. https://doi:10.1016/j.jclepro.2019.118213.

Ghalehnovi M, Shamsabadi E A, Khodabakhshian A, et al. (2019), Self-compacting architectural concrete production using red mud. Construction and building materials, 226: 418-427. https://doi:10.1016/j.conbuildmat.2019.07.248.

Ortega J M, Cabeza M, Tenza-Abril A J, et al. (2019). Effects of red mud addition in the microstructure, durability and mechanical performance of cement mortars. Applied Sciences, 9(5): 984. https://doi:10.3390/app9050984

Manfroi E. P., Cheriaf M., & Rocha J. C.(2014). Microstructure, mineralogy and environmental evaluation of cementitious composites produced with red mud waste. Construction and Building Materials, 67: 29-36. https://doi:10.1016/j.conbuildmat.2013.10.031.

Matos P R, Oliveira A L, Pelisser F, et al. (2018). Rheological behavior of Portland cement pastes and self-compacting concretes containing porcelain polishing residue. Construction and building materials, 175: 508-518. https://doi:10.1016/j.conbuildmat.2018.04.212.

Steiner L. R., Bernardin A. M., & Pelisser F. (2015). Effectiveness of ceramic tile polishing residues as supplementary cementitious materials for cement mortars. Sustainable Materials & Technologies, 4:30-35. https://doi:10.1016/j.susmat.2015.05.001.

Liu J, Wang D. (2017). Influence of steel slag-silica fume composite mineral admixture on the properties of concrete. Powder technology, 320: 230-238. https://doi:10.1016/j.powtec.2017.07.052.

Nemec J, Gandel R, Jerabek J, et al. Properties of selected alkali-activated materials for sustainable development[J]. Civil and Environmental Engineering, 2024, 20(1): 307-318. https://doi.org/10.2478/cee-2024-0024

Peknikova A, Jerabek J, Gandel R, et al. Physical–Mechanical Behavior of High-Performance Concrete and Ordinary Concrete with Portland Cement Mixtures After Exposure to Selected Durability Tests Including High Thermal Stress[J]. Buildings, 2025, 15(7): 1029. https://doi.10.3390/buildings15071029

Sun C, Chen L, Xiao J, et al. (2022). Effects of eco powders from solid waste on freeze-thaw resistance of mortar. Construction and Building Materials, 333: 127405. https://doi:10.1016/j.conbuildmat.2022.127405.

Jin J, Liu T, Li M, et al. (2024). Influence of biomass fly ash on durability of self-consolidating cement-tailings grout: Resistance to freeze-thaw cycles and sulfate attack. Journal of Building Engineering, 93: 109842. https://doi:10.1016/j.jobe.2024.109842.

Xu P, Guo Y, Zheng M, et al. (2024). Effect of Calcination Temperature on Polymerized Aluminum Chloride Waste Residue Cement Mortar. ACI Materials Journal, 121(6): 77-84. https://doi:10.14359/51743283.

Xu, P., Tong, J., & Shi R. (2024). The mechanical and frost resistance properties of pressed concrete blocks mixed with the polymeric aluminum chloride waste residue. Scientific Reports, 14(1): 12128. https://doi:10.1038/s41598-024-61347-1.

Xu, P., Guo. Y., Ding Y, et al. (2025). Effect of polymeric aluminum chloride waste residue and citric acid on the properties of magnesium oxychloride cement. Journal of Building Engineering, 101(000). https://doi:10.1016/j.jobe.2025.111864.

Yang, W., Hou, Z., He H, et al. (2022). Effect of Particle Size and Dosing of Polymeric Aluminum Chloride Waste Residue on Cement Mortar. Geofluids, 2022(1): 9675715. https://doi:10.1155/2022/9675715.

Chen Jianzhong. (1989). Determination of pore structure parameters of concrete by water absorption dynamics. Concrete and Reinforced Concrete, (06):9-13. https://doi:CNKI:SUN:HLTF.0.1989-06-001.

Hansen, S., & Sadeghian P. (2020). Recycled gypsum powder from waste drywalls combined with fly ash for partial cement replacement in concrete. Journal of Cleaner Production, 274: 122785. https://doi:10.1016/j.jclepro.2020.122785.

Wijaya, M. F., Ismanti, S., & Satyarno, I. Physical and Mechanical Properties of Fly Ash-Bottom Ash Geopolymer Mixtures on Expansive Clay Soil Stabilization as a Subgrade Material[J]. Civil and Environmental Engineering, 2024, 20(2): 890-904. https://doi.org/10.2478/cee-2024-0065.

How to Cite This Article

Yao, M., Lian, H., Chai, S., Shang, H., & Feng, T. (2026). The Effect of Polyaluminum Chloride (PAC) Residue on the Mechanical Properties and Freeze-Thaw Resistance of Cement Mortar. Civil and Environmental Engineering, 0 (0). https://doi.org/10.2478/cee-2026-0052